

## IMAGING SPECTROSCOPY OF TESPEL CLOUD IN LHD

I.A. Sharov, I.V. Miroshnikov, <sup>\*</sup>N. Tamura, V.Yu. Sergeev, <sup>\*</sup>S. Sudo, <sup>\*\*</sup>B.V. Kuteev

*SPbSPU, St. Petersburg, RF, e-mail: [sergeev@phtf.stu.neva.ru](mailto:sergeev@phtf.stu.neva.ru)*

*<sup>\*</sup>NIFS, Toki, Japan, e-mail: [ntamura@LHD.nifs.ac.jp](mailto:ntamura@LHD.nifs.ac.jp), [sudo.shigeru@LHD.nifs.ac.jp](mailto:sudo.shigeru@LHD.nifs.ac.jp)*

*<sup>\*\*</sup> RRC Kurchatov Institute, Moscow, RF, e-mail: [kuteev@nfi.kiae.ru](mailto:kuteev@nfi.kiae.ru)*

**Introduction.** Spatial distribution of plasma parameters and radiation in the pellet vicinity is highly needed for the further development of plasma-pellet interaction models and pellet applications for plasma fueling, control and diagnostics. Previous studies have demonstrated the approximate linear dependence of the averaged pellet cloud density on the ablation rate for both hydrogen [1] and polystyrene [2] pellets. This report is devoted to the study of polystyrene pellet clouds in the Large Helical Device. The observation of the pellet cloud radiation was performed using a 9 channel filter-lens imaging polychromator (NIOS) [3, 4]. The recent improvement of the NIOS setup allowed us to obtain and analyze dependencies of the 2D electron temperature and density distributions on both the pellet ablation rate and the ambient plasma density and temperature.

**Experimental setup.** In the experiments, snap-shots of sight-line integrated pellet cloud images were obtained simultaneously through interference filters in 9 spectral intervals with 10-30  $\mu$ s exposure time, which is much shorter than a typical pellet ablation time, 0.4-0.6 ms. Assuming that a cigar-like pellet cloud shape elongated along the local magnetic field lines, the cloud images were processed using Abel inversion procedure to determine local radiation distributions  $I_\lambda(r,z)$ , in cylindrical co-ordinates where  $z$  is oriented along the pellet cloud axis, i.e. parallel to the magnetic field line. Seven filters with narrow spectral characteristics ( $\sim 0.3$  nm of bandwidth) were used to get the 2D local distributions of the cloud electron density from the width of Stark broadened Balmer-beta line[4]. The electron temperature was determined from a ratio of the intensities of –Balmer-beta line emission and the continuum [4] using images obtained through the other two filters.

Previously reported data [4] were measured with a filter set which was not optimized. It led to the underestimation of the Balmer-beta line width and consequently to that of the pellet cloud electron density. This problem was resolved with the new filter set (see Table 1) which enables to measure higher cloud electron densities up to  $2 \times 10^{23} \text{ m}^{-3}$ . This setup was used to obtain cloud images of the 900-microns-diameter polystyrene pellet with an approximately 500-m/s velocity for a wide range of the target plasma parameters: ambient plasma density

$(1-5) \times 10^{19} \text{ m}^{-3}$ , temperature (0.8-1.5) keV and pellet ablation rate  $(1-12) \times 10^{22} \text{ atoms/s}$ . The polystyrene pellets were injected into the NBI-heated plasmas of LHD. The absorbed powers of co- and counter NBIs were nearly balanced.

Table 1. Parameters of the interference filters in the NIOS:

Filter	Stark №1	Stark №2	Stark №3	Stark №4	Stark №5	Stark №6	Stark №7	Cont.	$H_{\beta}$ full
Central WL, nm	482.7	484.3	485.39	485.60	485.78	486.12	486.94	630.45	486.5
FWHM, nm	0.26	0.28	0.34	0.30	0.27	0.31	0.31	4.95	10.
Aperture $\varnothing$ , mm	9.0	5.0	3.9	3.6	3.6	3.4	3.9	3.5	1.0

WL –wavelength, FWHM - Full Width on Half Magnitude

**Results and discussion.** Examples of the radial distributions of ablation rate, ambient plasma electron density and temperature are shown in Fig.1 for the shots #97812, #97816 with dramatically-different ambient plasma densities: the bulk plasma parameters during camera triggering were  $T_{epl} = 1.1 \text{ keV}$ ,  $N_{epl} = 1.6 \times 10^{19} \text{ m}^{-3}$ ,  $P_{NBI} = 9.3 \text{ MW}$ ,  $dN_H/dt = 2.5 \times 10^{22} \text{ atoms/s}$  in #97812 and  $T_{epl} = 1.1 \text{ keV}$ ,  $N_{epl} = 4.6 \times 10^{19} \text{ m}^{-3}$ ,  $P_{NBI} = 13.4 \text{ MW}$ ,  $dN_H/dt = 3.9 \times 10^{22} \text{ atoms/s}$  in #97816 respectively.

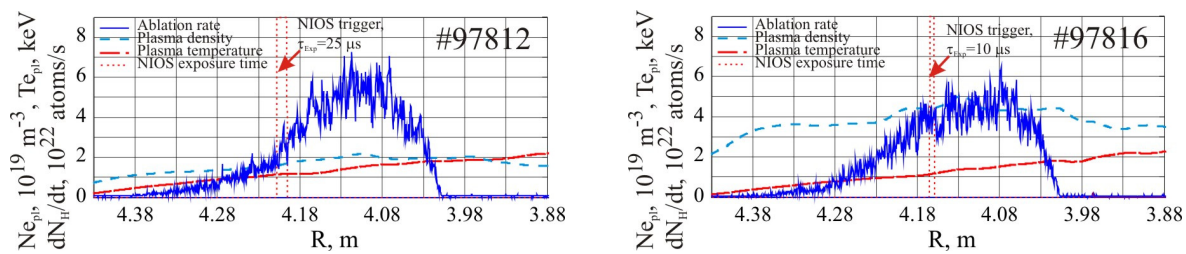


Fig. 1 Radial distributions of the ablation rate and ambient plasma parameters in LHD shots #97812 and #97816.

The trigger time and the exposure duration of the NIOS are shown by vertical dashed lines in Fig. 1. The distributions in both longitudinal and radial directions of the electron density and temperature in the pellet cloud are shown in Fig. 2 for the same shots as in Fig. 1.

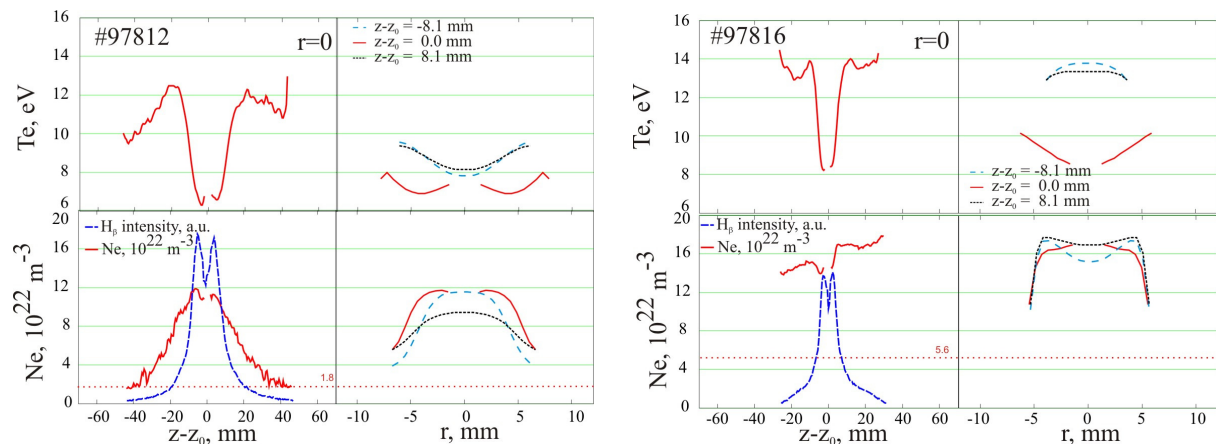


Fig 2. Profiles of pellet cloud electron temperature and density for the shot #97812 (low density plasma), #97816 (high density plasma).

As can be seen in Fig. 2, the measured cloud sizes increase with decreasing the ambient plasma density. The cloud temperature rises from 6-7 eV in the pellet vicinity to 10-12 eV at a large distance from the pellet. Maximal cloud densities are at the values of  $(1.2\text{-}1.6) \times 10^{23} \text{ m}^{-3}$ . The evaluated pellet cloud densities show the different behavior, although the Balmer-beta line intensities decrease with distance from the vicinity of the pellet cloud center in both cases. In the case with lower ambient plasma density the decay length is about 15 mm in the longitudinal direction. In the case with higher ambient plasma density there is a small density variation in the pellet cloud region within 10-20 mm in the longitudinal direction.

A dependence of cloud structure on the ablation rate of pellet material was also investigated. Experimental results with drastically-different ablation rates but similar bulk plasma parameters are shown in Fig.3 and Fig.4. The bulk plasma parameters during camera triggering were  $T_{epl} = 1.1 \text{ keV}$ ,  $N_{epl} = 1.6 \times 10^{19} \text{ m}^{-3}$ ,  $P_{NBI} = 9.3 \text{ MW}$ ,  $dN_H/dt = 2.5 \times 10^{22} \text{ atoms/s}$  in #97812 and  $T_{epl} = 1.6 \text{ keV}$ ,  $N_{epl} = 2.1 \times 10^{19} \text{ m}^{-3}$ ,  $P_{NBI} = 9.3 \text{ MW}$ ,  $dN_H/dt = 5.0 \times 10^{22} \text{ atoms/s}$  in #97814.

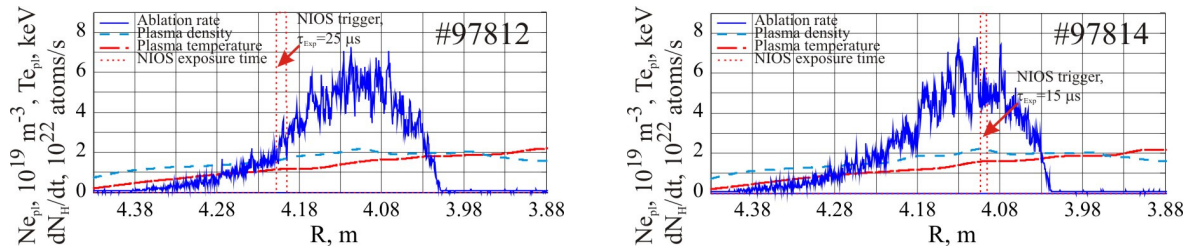


Fig. 3 Radial distributions of the ablation rate and ambient plasma parameters in LHD shots #97812 and #97814 with low ambient plasma electron density.

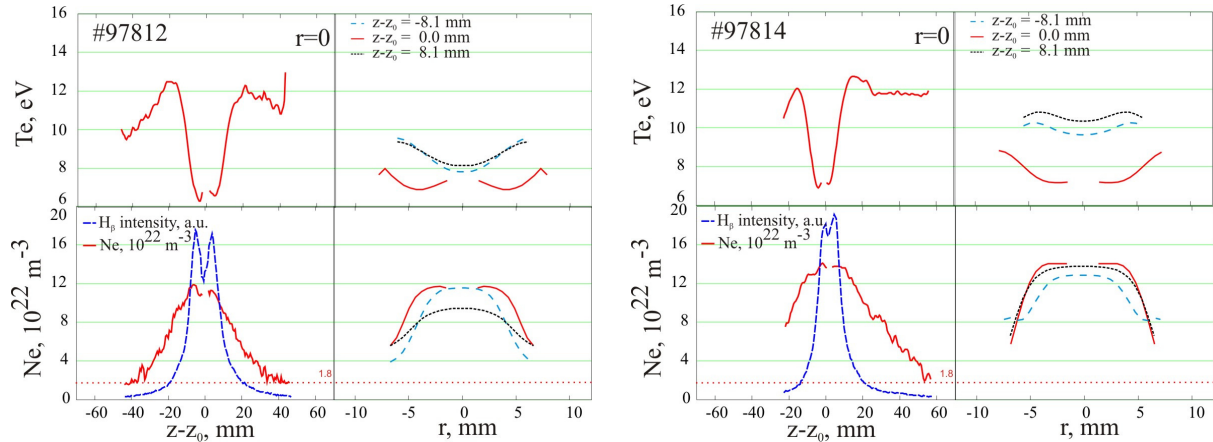


Fig. 4 Profiles of pellet cloud electron temperature and density for the shots #97812, #97814

One can see that the spatial distributions of the pellet cloud parameters didn't change significantly, though the ablation rate changed by a factor of two. It should be noted here that in the case of high density discharges the same situation was always observed.

**Summary.** The 2D distributions of the electron temperature and density in the polystyrene pellet cloud were obtained simultaneously in a wide range of the ambient plasma

parameters. The longitudinal profile of electron temperature in the clouds has a zone with fast temperature growth (from 5-7 eV to 10-11 eV) and a plateau zone. These values are obtained under assumption that carbon contribution into continuum radiation is equal to hydrogen one. An accurate calculations of continuum intensity accounting different ionization states of carbon ions may reduce the reported values of electron temperature by a factor of 3.

The measured electron density distributions in the ablating polystyrene pellet cloud show the different behavior depending on the ambient plasma density. In the lower density plasmas, there is a decay of the electron density along the magnetic field line. The decay length is much longer than the growth length of electron temperature. In higher density plasmas, the electron density in the cloud was higher than that in the lower density plasma and almost no decay of that was observed.

The spatial distributions of electron density and temperature in the polystyrene pellet cloud are mainly influenced by the ambient plasma density rather than the ambient plasma temperature and the pellet ablation rate. A similar dependence of the carbon cloud size on bulk plasma density was also detected in pellet experiments on W7-AS [5]

**Acknowledgements.** The work was supported by RFBR grant #08-02- 01372-a, a Grant-in-Aid for Scientific Research (B) (19340179) from Japan Society for the Promotion of Science, a Grant-in-Aid for Young Scientist (B) (19740349) from MEXT Japan, a budgetary Grant-in-Aid (NIFS09ULHH510) from NIFS, a project of Formation of International Network for Scientific Collaborations (NIFS09KEIN1018) of NIFS/NINS, Scholarship of the Russian Federation President for studying abroad in 2008/2009 year and Grant of Saint-Petersburg government for students and post-graduate students in 2009 year.

## References

- [1]. D. H. McNeil, et. al., Phys. Fluids B, Vol. 3, No. 8, August 1991, pp 1994-2009
- [2]. N. Tamura et.al., 30-th EPS Conference on Plasma Phys., St-Petersburg, 2003 Russia, P-1\_59
- [3]. N. Tamura et.al., Rev.Sci.Instrum. (2008) 79, No.10, 10F541
- [4]. I. V. Miroshnikov et.al., 36-th EPS Conference on Plasma Phys., Sofia, 2009, Bulgaria, P1.171, ([http://epsppd.epfl.ch/Sofia/pdf/P1\\_171.pdf](http://epsppd.epfl.ch/Sofia/pdf/P1_171.pdf))
- [5]. O.A. Bakhareva et.al., Plasma Physics Reports, Vol.31, No. 4, 2005, pp. 282-291